Inelastic proton scattering at 200 to 400 MeV for ^{24}Mg and ^{28}Si in a microscopic framework

K. H. Hicks,[a] R. G. Jeppesen,[b] C. C. K. Lin,[b] R. Abegg,[a] K. P. Jackson,[a] O. Häusser,[a],[b]
J. Lisantti,[c] C. A. Miller,[a] E. Rost,[d] R. Sawafta,[e] M. C. Vetterli,[a] and S. Yen[a]
[a]*TRIUMF, Vancouver, British Columbia, Canada V6T 2A3*
[b]*Simon Fraser University, Burnaby, British Columbia, Canada V5A 1S6*
[c]*University of Oregon, Eugene, Oregon 97403*
[d]*University of Colorado, Boulder, Colorado 80309*
[e]*University of Alberta, Edmonton, Alberta, Canada T6G 2J1*
(Received 14 December 1987)

Cross sections and analyzing powers for ^{24}Mg at 250 MeV and for ^{28}Si at 200 and 250 MeV, and cross sections for ^{28}Si at 400 MeV are presented for elastic scattering and inelastic scattering to the low-lying 2^+ state in each nucleus. The data are compared to "consistent" microscopic distorted-wave impulse approximation calculations in both relativistic and nonrelativistic models. The calculations presented here give a good description of the data. For comparison, calculations are also presented for previously published data on ^{12}C at 200, 250, and 400 MeV.

I. INTRODUCTION

The low-lying 2^+ states in many even-even nuclei observed in proton scattering experiments are frequently analyzed with a collective model because of the easily interpreted results and the good fits to the data. Few studies of these states have been done with a microscopic reaction model (such as the distorted-wave impulse approximation, or DWIA), and most of these studies have used phenomenological optical potentials fit to elastic scattering. The present study analyzes some new data of low-lying excited states with $J^\pi = 2^+$ in s-d shell nuclei at proton energies of 200 to 400 MeV. We use a microscopic (parameter-free) optical model for elastic scattering and the DWIA with a shell-model transition density for inelastic scattering. Both relativistic (RIA) and nonrelativistic (NRIA, or NRDD with a density dependent interaction) models are used that have "explicit" exchange terms. For comparison, previous data on ^{12}C in the same energy range are analyzed using the same procedures.

Calculations of elastic proton scattering have recently made considerable advances. RIA models[1,2] have shown that elastic scattering data (cross sections, A_y, and Q) are in excellent agreement with parameter-free calculations[2,3] for a wide range of spherical nuclei ($A = 16$ to 208) from proton energies of $T_p = 200$ to 800 MeV. NRDD model calculations do almost as well, but have trouble predicting[3,4] simultaneously both A_y and the spin-rotation parameter Q. Calculations of inelastic proton scattering have in general not been as successful. However, recent calculations for collective states in ^{12}C and ^{16}O at $T_p \simeq 150$ MeV using the NRDD model have shown great promise.[5-7] Similar analyses of collective states in ^{24}Mg and ^{28}Si at $T_p = 155$ MeV (using the NRDD model) also show good agreement with the data.[8] These calculations do well in part because transitions to these states are driven by the same parts of the effective N-N interaction (t_{NN}) as for elastic scattering (i.e., the isoscalar central and spin-orbit parts with a very small isoscalar tensor piece). It seems natural to extend these studies to higher energies where elastic calculations have enjoyed the most success, and to extend the study to RIA calculations which do so well for elastic scattering. If the inelastic calculations succeed, we will have tested the prescription of the RIA and NRIA (NRDD) Models. We can then examine other states with confidence in our reaction model. Comparison of calculations to data for other excited states with different spin and parity (and different isospin) will then provide tests of other components (e.g., isovector and/or tensor parts) of the effective proton-nucleus interaction, or tests of nuclear structure models.

Shell-model calculations for s-d shell nuclei have also been improved recently,[9] making this mass region ideal for nuclear structure studies. In particular, the low-lying $E2$ excitations have been studied in detail[10] showing good agreement for static quadrupole moments, provided an isoscalar effective charge of 0.35 is used. The effective charge describes core polarization, which accounts, in an approximate way, for transitions out of the s-d shell-model space. Analysis of electron scattering data (at nonzero momentum transfer q) with this model have further demonstrated its utility for low-lying 2^+ states.[9,11] The s-d shell is perhaps better suited for studies of inelastic proton scattering than the p shell, which apparently shows few-body effects[12] such as α clustering in ^{12}C. The shell model is expected to do well near the middle of the shell, where strongly collective states are reasonably described within the s-d valence space. Furthermore, the shell-model space required to fully describe larger model spaces, such as the f-p shell, is beyond present computational abilities.[13] All of this makes ^{28}Si and ^{24}Mg ideal for studies with inelastic proton scattering.

A recent publication[14] has compared microscopic DWIA calculations for the 3^- and 5^- states in ^{40}Ca at 362 MeV using both nonrelativistic and relativistic models. The NRIA calculations are in good agreement with the cross sections and forward angle A_y data, but poor

agreement with the A_y data at larger angles (past the first minimum). The relativistic calculations for these data did not use explicit exchange and are somewhat higher than the data at angles past 30°. The present study differs by using explicit exchange for the RIA calculations, and considers the 2^+ states of several different nuclei over a range of incident proton energies.

II. EXPERIMENT

Data were obtained on ^{28}Si with 200, 250, and 400 MeV protons, and for ^{24}Mg with 250 MeV protons, accelerated by the TRIUMF cyclotron. Targets of 17.2 and 20.5 mg/cm^2 thickness were used for ^{nat}Si and enriched ^{24}Mg, respectively. The scattered protons were detected with the medium resolution spectrometer (MRS).[15] The MRS has excellent ray-trace capabilities and produces spectra with minimal instrumental background down to very small angles (about 3°). Absolute differential cross sections were determined using a front-end wire chamber to determine the solid angle acceptance. The efficiency of all wire chambers was calculated from the built-in redundancy of the close-spaced wire chambers. The computer dead time was monitored by pulser events that were counted in free-running scalers and compared to the number of events seen in a coincidence register in the CAMAC electronics. The beam charge was determined with a copper beam stop (for angles less than 16°) or in a calibrated secondary emission monitor (for large angles). The beam polarization was monitored continuously using an in-beam polarimeter[16] with a thin (2.89 mg/cm^2) CH_2 target. This also provided a beam flux measurement that agreed with the charge integration to within an uncertainty of 1.5%. A CH_2 target was run to test the cross section normalization, and the resulting p-p elastic yield was compared to the cross section calculated from phase-shift analysis of the well known p-p scattering. The data have been multiplied by 1.05 to account for this difference, which is still within the systematic uncertainty of 6% (the error bars shown in the figures do not include this uncertainty). Full details of the data reduction are given in Ref. 17. Only data for the elastic and 2^+ states will be presented here. Previously published experimental results for ^{12}C at 200, 250, and 400 MeV taken at IUCF,[7,18] TRIUMF,[19] and LAMPF (Ref. 20) will also be shown for comparison.

III. CALCULATIONS

The RIA calculations were done with the computer code DREX (Ref. 21) which uses an effective interaction (t_{NN}) fit to the spring 1984 N-N phase shifts[22] as given by Horowitz.[23] Both the NRIA calculations, which use the t_{NN} given by Franey and Love,[24] and the NRDD calculations, which use the t_{NN} given by von Geramb,[25] were done with the computer code DW81.[26] We have done "consistent" calculations for all cases, using the same effective interaction for both elastic scattering (and thus, the distorted waves) and to induce the inelastic transitions. This prescription was found to give a better description of the A_y data in Ref. 5; similar sensitivities to the distorted waves were found in Ref. 7. As stated above, both codes calculate exchange terms explicitly, rather than approximately as in Ref. 5. In order to obtain some consistency between RIA and NRIA (NRDD) calculations, we have used the same ground-state density described by a fit to the electron scattering charge density with a Woods-Saxon (two-parameter Fermi) form.[27] This density was used for both protons and neutrons, which should be a good approximation for $N=Z$ nuclei. Similarly, all calculations used single-particle wave functions derived from a Woods-Saxon shaped potential, and one-body transition density matrix elements (transition amplitudes) from Ref. 9. The DREX calculations used these transition amplitudes with the prescription given in Ref. 21.

Careful checks were made in order to ensure compatibility with previous studies. The NRDD calculations for the 2^+ state of ^{12}C at 200 MeV of Ref. 7 were reproduced using DW81 (to within a few percent, except at the largest angles where numerical errors become important); these calculations are somewhat different from those presented here because Ref. 7 used harmonic oscillator wave functions and phenomenological optical potentials. Similarly, the NRIA calculations of Ref. 28 were reproduced using the earlier (1981) Love-Franey interaction and the phenomenological optical potential parameters given there. The RIA calculations use the same version of the DREX code as was used for Ref. 21. The microscopic optical potentials for the NRDD and NRIA were generated using the code MAINX8,[29] where the NRDD potentials have been multiplied by the ratio of reduced mass divided by reduced total energy as needed for use with a Schrödinger equation incorporating relativistic kinematics.[30]

IV. RESULTS AND DISCUSSION

Elastic scattering data for ^{24}Mg at 250 MeV are shown in Fig. 1 together with calculations in the NRIA, NRDD, and RIA models. All three models give a good description of both the cross section and A_y data forward of 40°, with a slight preference for the RIA calculation. The difference at large angles (large momentum transfer) may be due to the imperfect parametrization of the charge density used here. Data for ^{28}Si from the present measurements and from a previous measurement[31] at 134 MeV are shown in Fig. 2. The RIA model gives an excellent description of the cross section and A_y at 250 MeV and the cross section at 400 MeV; the NRIA and NRDD are almost as good. The 200 MeV results favor the nonrelativistic models, with the NRDD doing slightly better for the incomplete A_y data; the RIA is almost as good. At 134 MeV, all models describe the cross section reasonably well, with the NRDD model favored for the A_y (but this description is certainly not as good as at 250 MeV).

For comparison, previously published elastic scattering data[18–20] on ^{12}C at 200, 250, and 400 MeV are shown in Fig. 3. As for ^{28}Si, all three models do about as well at 200 MeV. None of the three models reproduce the large angle analyzing powers. At 250 MeV, all three models underpredict the cross section. This behavior is unexpected based on the excellent results for ^{24}Mg and ^{28}Si at

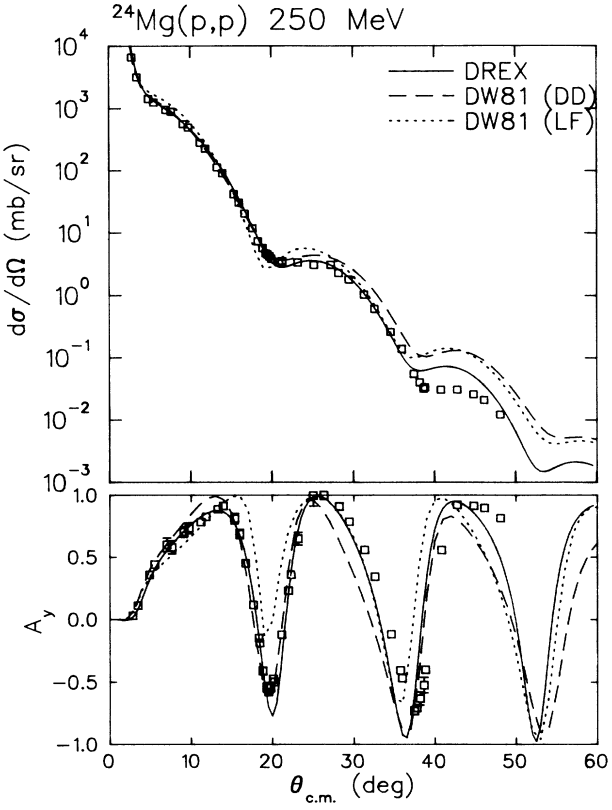

FIG. 1. Elastic proton scattering data for ^{24}Mg at 250 MeV. The solid lines represent calculations in the RIA model (using DREX) and the dashed or dotted lines represent calculations in the NRDD or NRIA models, respectively, (using DW81).

250 MeV, and no explanation is attempted. At 400 MeV the relativistic model is clearly favored. The calculated A_y for both ^{12}C and ^{28}Si at 400 MeV have similar shapes for the three models, but the A_y data for ^{12}C (which were lacking for ^{28}Si) clearly help discriminate between models. More A_y data at 400 MeV are needed, especially at larger angles. We note that RIA calculations for elastic scattering using Hartree densities[2] for ^{12}C at 200 MeV do not agree as well with the data as compared to empirical densities. We have also found this to be true[32] for the preceding data presented for the deformed nuclei ^{24}Mg and ^{28}Si.

In order to get consistent calculations for inelastic proton scattering, Woods-Saxon shaped potentials were used to generate single-particle wave functions. The nonrelativistic Woods-Saxon parameters were taken from Ref. 9 as determined by an extensive fit to elastic electron scattering data in the s-d shell. This prescription, which uses both the shape and depth of the potential, uniquely determines the binding energy for the bound states. The relativistic Woods-Saxon parameters were taken from Ref. 21 as determined by fits to electron scattering. This prescription fixes the binding energy (we used the values from Elton and Swift[33]) and searches on the well depth. Although these two methods differ in principle, the calculated inelastic electron scattering form factors are virtually identical (see below). The values of the inputs used for the present calculations are given in Table I.

The transition amplitudes used in the present study are given in Table II. The amplitudes for ^{28}Si and ^{24}Mg are from the shell model of Brown and Wildenthal,[9] and the amplitudes for ^{12}C are from the shell model of Cohen and Kurath.[34] Other studies have used more complex amplitudes for ^{12}C from an RPA model,[6,7] but have found the Cohen-Kurath representation with an overall normalization for core polarization to be just as good. Similar results are found for ^{24}Mg and ^{28}Si, but with small discrepancies at large momentum transfers.[8]

Electron scattering data are available[35,36] for the low-lying 2^+ states in ^{28}Si, ^{24}Mg, and ^{12}C which makes a good testing ground for the wave functions described above. Figure 4 shows these data along with the calculations from the electron scattering code ELECTL.[37] The curves have been multiplied by a factor of $(1.7)^2$ for ^{28}Si and ^{24}Mg, as needed for the effective charge of 0.35 for the neutron and 1.35 for the proton to account for core polarization.[10] The curves for ^{12}C have been multiplied by a factor of 2 as found in Ref. 36 to account for core polarization in the p shell. Although the electron scattering data do not cover as large a range of momentum transfers as the proton scattering data, we can feel confident about the normalization of these wave functions and about the nuclear structure input at low momentum transfer.

The inelastic proton scattering data are presented in Fig. 5 for ^{24}Mg at 250 MeV together with calculations from the three models previously discussed. The RIA model gives an excellent description of the data, with the NRDD almost as good. The NRDD calculation is noticeably better than the NRIA, although the signature of smaller cross section at small q and larger cross section at large q is not as clear as in Refs. 5, 6, and 8. Indeed, the NRIA gives a better description of the cross section data at large angles. This is attributed to the use of microscopic optical potentials, as we find this to significantly alter the ^{12}C calculations presented below. The A_y have the strong oscillations characteristic of the "consistent" calculations of Kelly[5] and show much better agreement with the data than calculations for collective states at lower energies using phenomenological optical models.[8,6]

We can examine the energy dependence of the calculations using the ^{28}Si data, which are shown in Fig. 6. As was the case for ^{24}Mg, the RIA prediction for ^{28}Si at 250 MeV is quite impressive, and the density-dependent effects are favored at angles less than 40° for the nonrelativistic models. All the ^{28}Si calculations slightly overpredict the peak cross section at all energies, and this may be due to the slightly higher form factor relative to ^{28}Si(e,e') data as compared to that for ^{24}Mg. At 134 and 200 MeV, all three models do reasonably well in describing the data, with a slight preference for the NRDD model, especially for the 134 MeV A_y data. However, at 400 MeV all three models miss the last diffraction maximum. This is not likely to be due to the nuclear structure input, even though this maximum is at a larger momentum transfer than for the (e,e') data, because the 250 MeV calculations agree with the data at the third diffraction maximum (at the same q). In addition, the

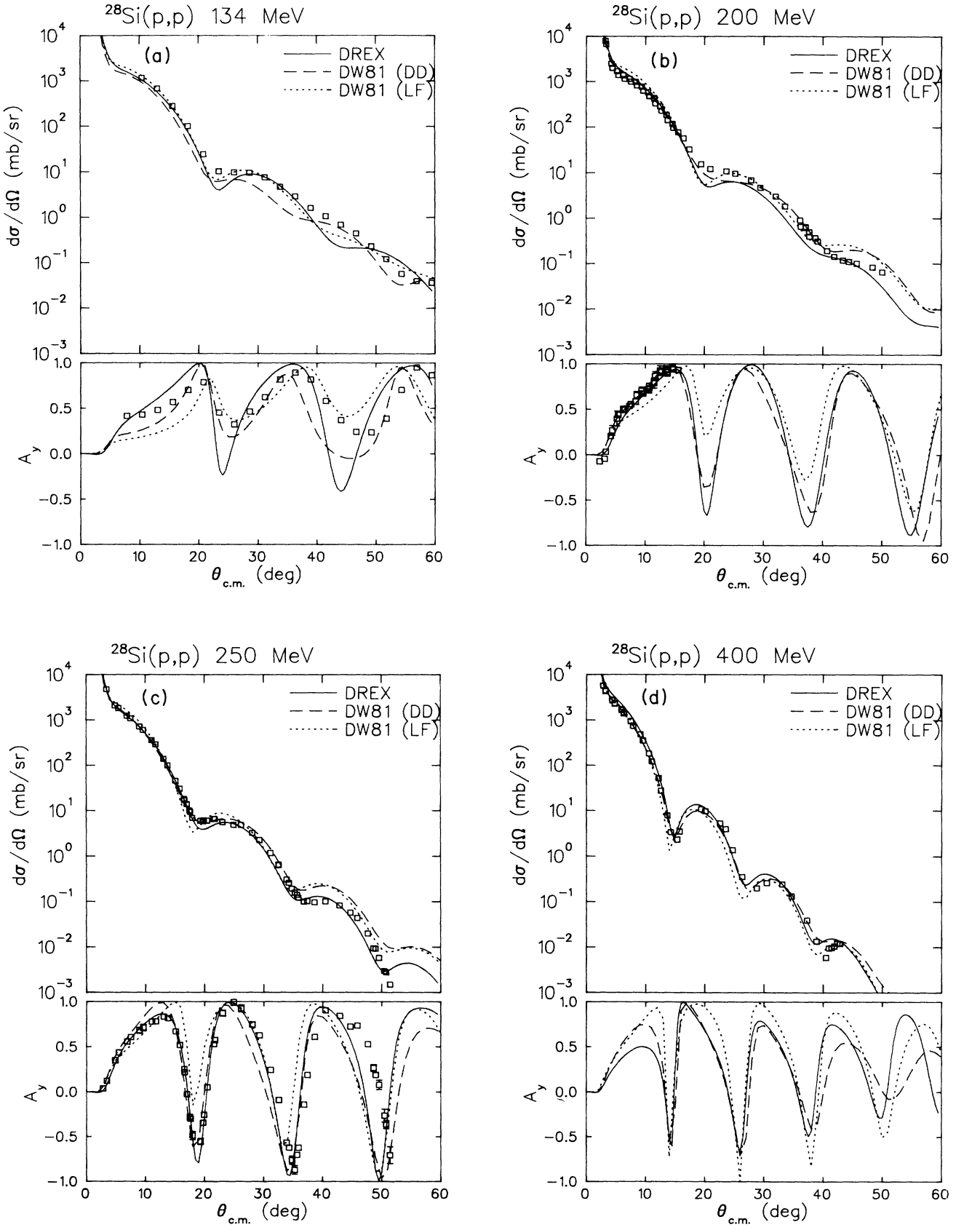

FIG. 2. Elastic proton scattering data for ^{28}Si at 134 MeV (from Ref. 31) and at 200, 250, and 400 MeV from the present work. For explanation of the curves, see Fig. 1.

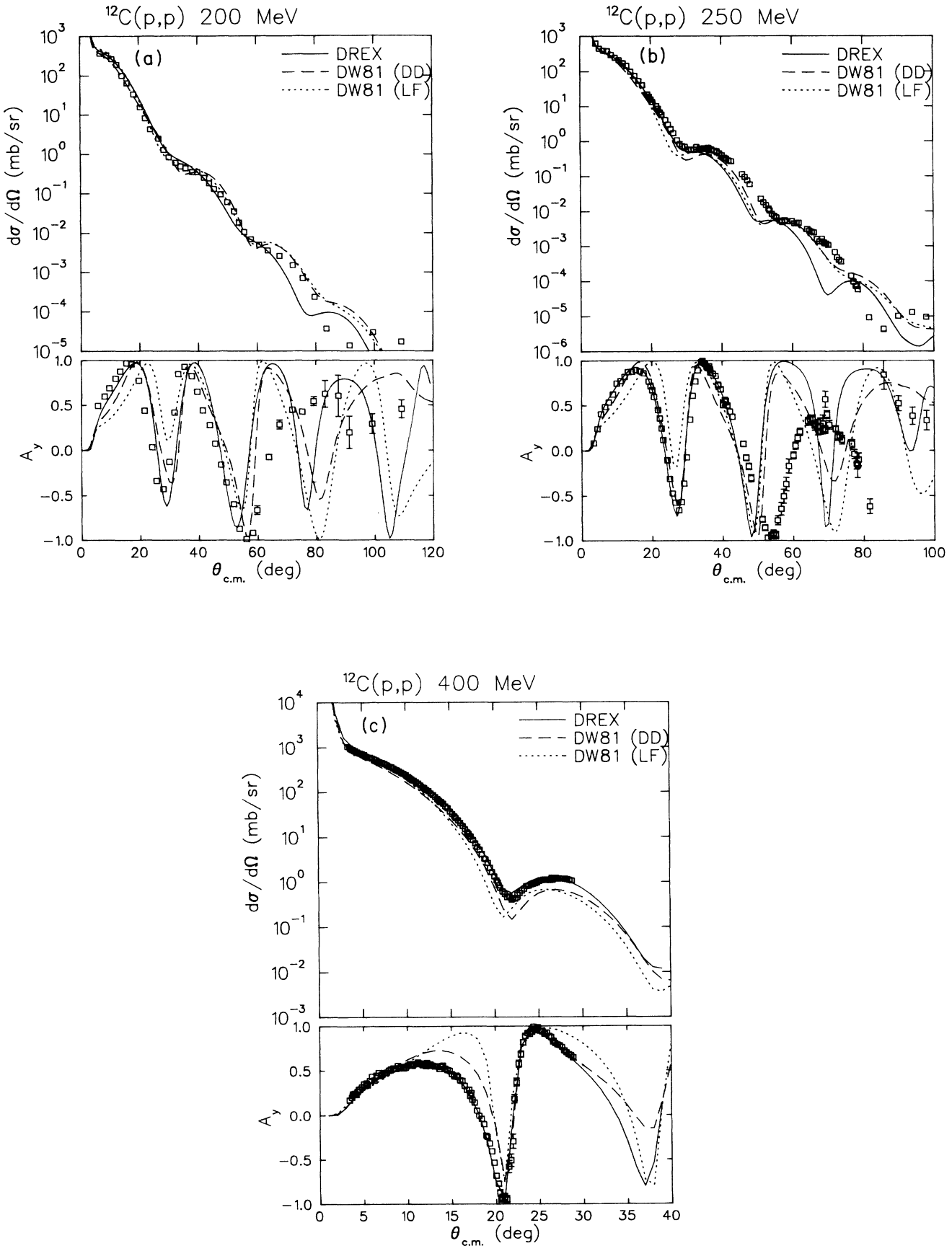

FIG. 3. Elastic proton scattering data for ^{12}C from Refs. 18–20. For explanation of the curves, see Fig. 1.

TABLE I. Standard inputs to calculations.

Input	Inputs to the DW81 code Description	Inputs to the DREX code Description
nonlocality	explicit exchange used	explicit exchange used
interaction	NRIA: (140,210,270,425) MeV set of Ref. 24 NRDD: (150,200,250,400) MeV set of Ref. 25 used for (134,200,250,400) MeV calculations	(135,200,200,400) MeV set of Ref. 21 used for (134,200,250,400) MeV calculations
kinematics	relativistic kinematics	relativistic kinematics
optical potential	input from MAINX8 with charge density parameters: $c=1.029$, $z=0.5224$, $w=-0.149$ (for ^{12}C) $c=1.020$, $z=0.538$ (for ^{24}Mg) $c=1.023$, $z=0.542$ (for ^{28}Si)	calculated internally with charge density parameters: $c=1.029$, $z=0.5224$, $w=-0.149$ for ^{12}C $c=1.020$, $z=0.538$ (for ^{24}Mg) $c=1.023$, $z=0.542$ (for ^{28}Si)
wave function	microscopic Woods-Saxon potential, with parameters: $V=-49.59$, $R=1.276$, $A=0.539$, $\lambda_{s,0}=21.1$ (for ^{12}C) $V=-50.95$, $R=1.288$, $A=0.621$, $\lambda_{s,0}=21.1$ (for ^{24}Mg) $V=-51.42$, $R=1.280$, $A=0.651$, $\lambda_{s,0}=21.1$ (for ^{28}Si)	microscopic Woods-Saxon potential, $R=1.275$, $A=0.635$ well depth determined from binding energy
binding energy	determined from above well depth	^{12}C: $\epsilon_{0p_{3/2}}=-15.4$, $\epsilon_{0p_{1/2}}=-9.7$ ^{24}Mg: $\epsilon_{0d_{5/2}}=-14.0$, $\epsilon_{1s_{1/2}}=-6.0$, $\epsilon_{0d_{3/2}}=-4.0$ ^{28}Si: $\epsilon_{0d_{5/2}}=-17.5$, $\epsilon_{1s_{1/2}}=-13.0$, $\epsilon_{0d_{3/2}}=-6.5$
amplitudes	see Table II (isospin representation)	see Table II (proton-neutron representation)

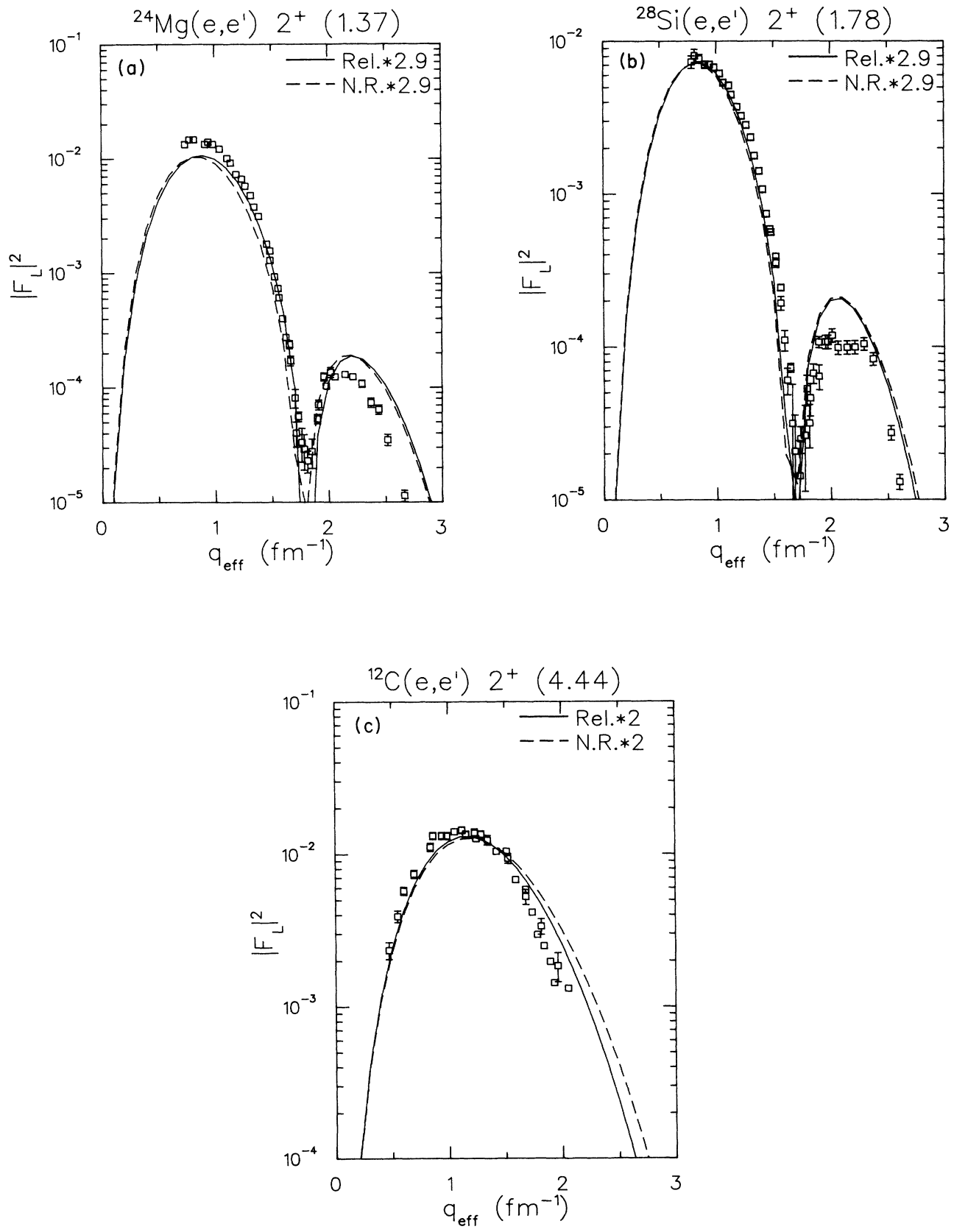

FIG. 4. Inelastic electron scattering data for the low-lying 2^+ state in ^{28}Si, ^{24}Mg, and ^{12}C from Refs. 35 and 36. The curves show results of calculations using Woods-Saxon wave functions with transition amplitudes given in Table II. The calculations have been multiplied by the factors shown to account for effective charge as described in the text.

TABLE II. Transition amplitudes.[a]

Particle	Hole	^{12}C	^{24}Mg	^{28}Si
$0p_{3/2}$	$0p_{3/2}$	−0.3097		
$0p_{3/2}$	$0p_{1/2}$	−0.5006		
$0p_{1/2}$	$0p_{3/2}$	+0.7594		
$0p_{5/2}$	$0d_{5/2}$		−0.6176	−0.2986
$0d_{5/2}$	$1s_{1/2}$		+0.3232	+0.4066
$0d_{5/2}$	$0d_{3/2}$		−0.3197	−0.3038
$1s_{1/2}$	$0d_{5/2}$		+0.4255	+0.5949
$1s_{1/2}$	$0d_{3/2}$		+0.1523	+0.0862
$0d_{3/2}$	$0d_{5/2}$		+0.3155	+0.3835
$0d_{3/2}$	$1s_{1/2}$		−0.1473	−0.1532
$0d_{3/2}$	$0d_{3/2}$		−0.0653	−0.1714

[a]From Refs. 9 and 34, but with a $(-1)^{\Delta n}$ phase convention where $\Delta n = n_2 - n_1$ is the change in the principle quantum number. The values are given in isospin representation; dividing by 1.414 gives values in proton-neutron representation.

400 MeV *elastic* calculations agree with the data at 40°, showing that the effective interaction is correct at this momentum transfer. It is likely that the off-shell description of the effective interaction is not described properly at this energy. This interpretation was suggested (provided coupled-channel effects are small[38]) in Ref. 7 where the influence of different off-shell parametrizations of the NRDD effective interaction are discussed for the low-lying 2^+ state in ^{12}C at proton energies below 200 MeV. The 400 MeV data shown in Fig. 6 could be a good testing ground for improvements to the off-shell descriptions of the effective interaction. As is the case for elastic scattering, more inelastic data with analyzing powers are needed at 400 MeV, especially at larger angles where the momentum transfers probe parts of t_{NN} that cannot be reached by N-N scattering.

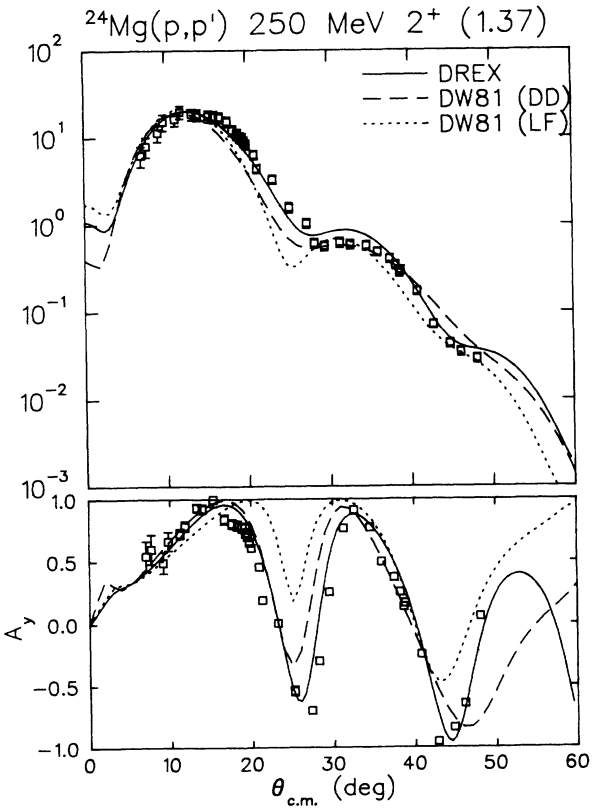

FIG. 5. Inelastic proton scattering data for the low-lying 2^+ state in ^{24}Mg. The curves use the same models as in Fig. 1. The calculations have been multiplied by $(1.7)^2$ to account for core polarization as determined by Ref. 10.

For comparison, Fig. 7 shows inelastic proton scattering data[7,19,20] for ^{12}C. At 200 MeV, the NRDD calculations are similar to those published earlier[6,7] using harmonic oscillator wave functions and phenomenological optical model distortions. However, we find that the NRIA calculations are in good agreement with the data, in contrast to the previous calculations.[28] We have found that the newer parameterization given by Franey and Love[24] has only a small effect on these calculations compared to the earlier parameter set given by Love and Franey. Similarly, the use of Woods-Saxon wave functions as compared to harmonic oscillator wave functions makes little difference. The significant differences between previous calculations and the present ones are attributed to using phenomenological optical potentials compared to microscopic ones. This is important, as these differences have in the past been attributed to density-dependent effects. However, none of the three models show the kind of agreement with the A_y data as was found for ^{24}Mg and ^{28}Si at 250 MeV. This may be due to the nuclear structure input, as electron scattering data with only $q < 2$ fm^{-1} are available (or the equivalent of about 40° for the 200 MeV ^{12}C data in Fig. 7). Large scale RPA transition densities exist for this state,[6] but have little effect on the shape of the calculated cross section, except to increase the normalization so that no effective charge is needed. Our own calculations (not shown) confirm this, and show very little effect on A_y. At 400 MeV, the RIA and NRIA give the best description for the cross section, while the NRDD is perhaps better for the A_y data over the limited angular range of the data.

The ^{12}C data are the only sets to go out in angle beyond 60°, where the approximations used in the calculations appear to break down. Any of several effects could be causing this. Two-step processes become more important as the momentum transfer increases, and this is the most likely cause. As mentioned earlier, off-shell parts of the interaction can have a measureable effect at the larger angles. Nuclear structure effects might also play a role. The calculations used in the present study should not be applied to scattering angles beyond 60 deg without modifications for two-step contributions.

V. CONCLUSIONS

The data presented here are described well by all three models, with a preference for the RIA above 200 MeV. Care has been taken to give both relativistic and nonrelativistic models similar inputs, with the nuclear structure

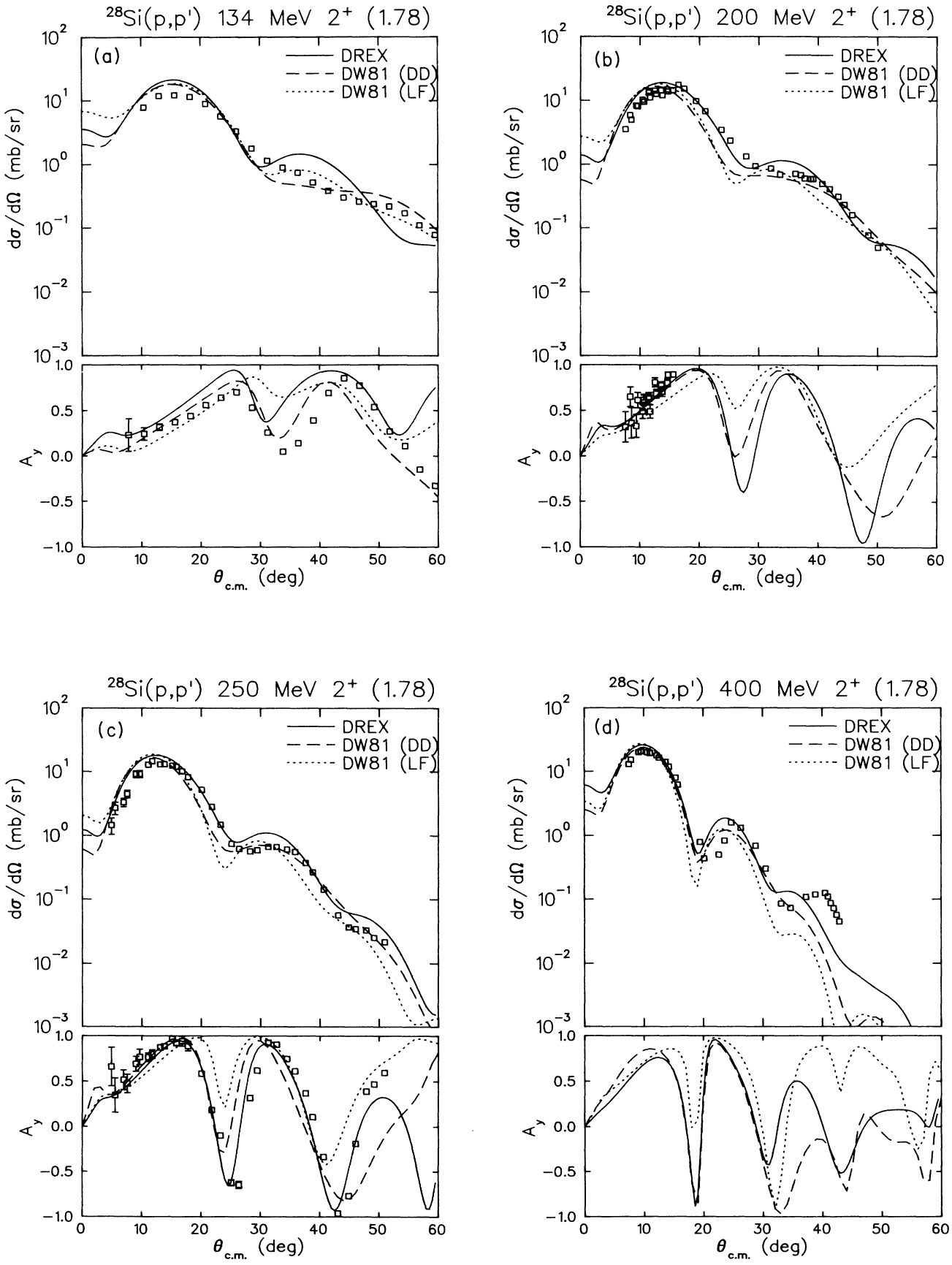

FIG. 6. Inelastic proton scattering data for the low-lying 2$^+$ state in ^{28}Si. For explanation of the curves, see Fig. 5.

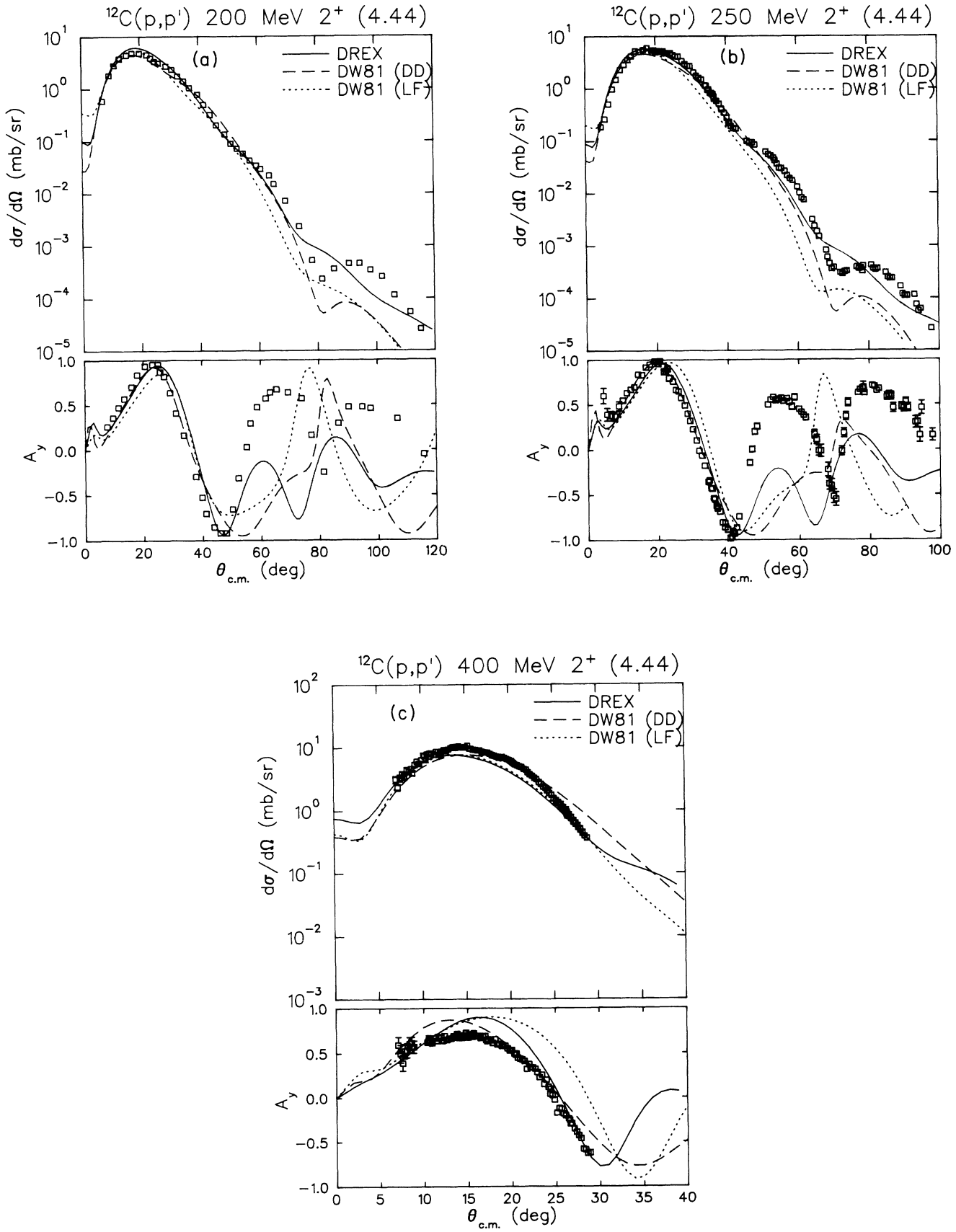

FIG. 7. Inelastic proton scattering data for the low-lying 2$^+$ state in ^{12}C. The curves use the same models as in Fig. 1. The calculations have been multiplied by a factor of 2 as determined by Ref. 36.

input guided by comparisons to elastic and inelastic electron scattering. The elastic proton scattering data are described well enough to justify using a "consistent" calculation where the same effective interaction is used for the distorted waves as that used to induce the inelastic transition.

Calculations for inelastic proton scattering to low-lying collective states in the *p*- and *sd*-shell are rapidly becoming as predictive as calculations for elastic proton scattering, in both relativistic and nonrelativistic models. This suggests that we can have confidence in the prescriptions used for the RIA and NRIA (NRDD) models. Because transitions to low-lying 2^+ states are induced by the same parts of the effective interaction as are important for elastic scattering, data at large angles coupled with (e,e') data at larger momentum transfers may be useful in testing different representations of the off-shell pieces of the N-N interaction. Furthermore, comparison between data for other excited states and calculations with these models, where the nuclear structure can be completely tested by (e,e') data, will be a good test of other parts of the effective interaction. As an example, the data of Olmer[39] on stretched states in ^{28}Si show that the isoscalar and isovector tensor parts of the proton-nucleus force are not well represented by the nonrelativistic effective interaction below 200 MeV. Clearly, improved parametrizations of t_{NN} will be needed in the near future to compare with the high-quality data which are being produced at intermediate energy facilities, even where transition densities are taken directly from electron scattering results rather than from shell-model or RPA calculations.

ACKNOWLEDGMENTS

The authors thank the TRIUMF staff for their efforts in delivering high-quality polarized beam. We thank C. Glashausser, D. McDaniels, and B. Jennings for valuable comments on the text. Special thanks to H.-O. Meyer and K. Jones for providing the ^{12}C data. This work was supported by grants from the National Science and Engineering Council of Canada.

[1]J. R. Shepard, J. A. McNeil, and S. J. Wallace, Phys. Rev. Lett. **50**, 1443 (1983); J. A. McNeil, J. R. Shepard, and S. J. Wallace, *ibid.* **50**, 1439 (1983).
[2]D. P. Murdock and C. J. Horowitz, Phys. Rev. C **35**, 1442 (1987).
[3]L. Ray and G. W. Hoffmann, Phys. Rev. C **31**, 538 (1985).
[4]O. Hausser *et al.*, Phys. Lett. **184B**, 316 (1987).
[5]J. Kelly *et al.*, Phys. Rev. Lett. **45**, 2012 (1980).
[6]W. Bauhoff *et al.*, Nucl. Phys. **A410**, 180 (1983).
[7]M. Hugi, W. Bauhoff, and H. O. Meyer, Phys. Rev. C **28**, 1 (1983).
[8]K. Amos and W. Bauhoff, Nucl. Phys. **A424**, 60 (1984).
[9]B. A. Brown, R. Radhi, and B. H. Wildenthal, Phys. Rep. **101**, 313 (1983).
[10]M. Carchidi, B. H. Wildenthal, and B. A. Brown, Phys. Rev. C **34**, 2280 (1986).
[11]S. Yen *et al.*, Phys. Lett. **124B**, 471 (1983).
[12]W. Bauhoff, H. Schultheis, and R. Schultheis, Phys. Rev. C **29**, 1046 (1984).
[13]B. A. Brown, private communication.
[14]D. Frekers *et al.*, Phys. Rev. C **35**, 2236 (1987).
[15]C. A. Miller, in *Studying Nuclei with Medium Energy Protons*, TRIUMF Report No. TRI-83-3, p. 339 (unpublished).
[16]R. Abegg and R. Schubank, TRIUMF design note TRI-DN-87-17.
[17]C. C. K. Lin, M. Sc. thesis, Simon Fraser University, 1987.
[18]H. O. Meyer *et al.*, Phys. Rev. C **23**, 616 (1981); **24**, 1782 (1981).
[19]H. O. Meyer *et al.* Phys. Rev. C **37**, 544 (1988).
[20]K. Jones, Ph.D. thesis, Rutgers University, 1984, LAMPF Report No. LA-10064-T.
[21]E. Rost, code DREX (unpublished); E. Rost *et al.*, Phys. Rev. C **35**, 681 (1987).
[22]R. A. Arndt and L. S. Roper, code SAID (unpublished).
[23]C. Horowitz, Phys. Rev. C **31**, 1340 (1985).
[24]M. A. Franey and W. G. Love, Phys. Rev. C **31**, 488 (1985).
[25]H. V. von Geramb and K. Nakano, in *The Interaction Between Medium Energy Nucleons in Nuclei*, AIP Conf. Proc. No. 97, edited by H. O. Meyer (AIP, New York, 1983) p. 44.
[26]R. Schaeffer and J. Raynal, Code DWBA70 (unpublished); J. Comfort, extended version DW81 (unpublished).
[27]C. W. de Jager, H. de Vries, and C. de Vries, At. Data Nucl. Data Tables **14**, 479 (1974).
[28]J. R. Comfort *et al.*, Phys. Rev. C **26**, 1800 (1982).
[29]Code MAINX8, modified by R. G. Jeppesen (unpublished).
[30]Ma Ji, M. Sc. thesis, Simon Fraser University, 1987; Ma Ji *et al.* (unpublished); L. Lee, Ph.D. thesis, University of Toronto, 1987.
[31]S. Yen, Ph.D. thesis, University of Toronto, 1983.
[32]D. P. Murdock, private communication.
[33]L. R. B. Elton and A. Swift, Nucl. Phys. **A94**, 52 (1967).
[34]S. Cohen and D. Kurath, Nucl. Phys. **73**, 1 (1965); T. H. S. Lee and D. Kurath, Phys. Rev. C **21**, 293 (1980).
[35]G. C. Li, M. R. Yearian, and I. Sick, Phys. Rev. C **9**, 1861 (1974).
[36]J. B. Flanz *et al.*, Phys. Rev. Lett. **41**, 1642 (1978).
[37]J. R. Shepard, code ELECTL (unpublished).
[38]G. S. Blanpied *et al.*, Phys. Rev. C **25**, 422 (1982), and references therein.
[39]C. Olmer *et al.*, Phys. Rev. C **29**, 361 (1984).